JOURNAL OF BACTERIOLOGY, June 2005, p. 3825–3832 Vol. 187, No. 11
0021-9193/05/$08.00+0 doi:10.1128/JB.187.11.3825–3832.2005
Copyright © 2005, American Society for Microbiology. All Rights Reserved.

Analysis of Transient Polyhydroxybutyrate Production in *Wautersia eutropha* H16 by Quantitative Western Analysis and Transmission Electron Microscopy

Jiamin Tian,[1] Aimin He,[1] Adam G. Lawrence,[2] Pinghua Liu,[1] Nicki Watson,[3] Anthony J. Sinskey,[2] and JoAnne Stubbe[1,2]*

Departments of Chemistry[1] and Biology,[2] Massachusetts Institute of Technology, Cambridge, Massachusetts 02139, and Whitehead Institute for Biomedical Research, 9 Cambridge Center, Cambridge, Massachusetts 02142[3]

Received 8 November 2004/Accepted 12 January 2005

Polyhydroxybutyrates (PHBs) are polyoxoesters generated from (*R*)3-hydroxybutyryl coenzyme A by PHB synthase. During the polymerization reaction, the polymers undergo a phase transition and generate granules. *Wautersia eutropha* can transiently accumulate PHB when it is grown in a nutrient-rich medium (up to 23% of the cell dry weight in dextrose-free tryptic soy broth [TSB]). PHB homeostasis under these growth conditions was examined by quantitative Western analysis to monitor the proteins present, their levels, and changes in their levels over a 48-h growth period. The proteins examined include PhaC (the synthase), PhaP (a phasin), PhaR (a transcription factor), and PhaZ1$_a$, PhaZ1$_b$, and PhaZ1$_c$ (putative intracellular depolymerases), as well as PhaZ2 (a hydroxybutyrate oligomer hydrolase). The results show that PhaC and PhaZ1$_a$ were present simultaneously. No PhaZ1$_b$ or PhaZ1$_c$ was detected at any time throughout growth. PhaZ2 was observed and exhibited an expression pattern different from that of PhaZ1$_a$. The levels of PhaP changed dramatically and corresponded kinetically to the levels of PHB. Transmission electron microscopy (TEM) provided the dimensions of the average cell and the average granule at 4 h and 24 h of growth (J. Tian, A. J. Sinskey, and J. Stubbe, J. Bacteriol. 187:3814–3824, 2005). This information allowed us to calculate the amount of each protein and number of granules per cell and the granule surface coverage by proteins. The molecular mass of PHB (10^6 Da) was determined by dynamic light scattering at 4 h, the time of maximum PHB accumulation. At this time, the surface area of the granules was maximally covered with PhaP (27 to 54%), and there were one or two PhaP molecules/PHB chain. The ratio of PHB chains to PhaC was ~60, which required reinitiation of polymer formation on PhaC. The TEM studies of wild-type and Δ*phaR* strains in TSB provided further support for an alternative mechanism of granule formation (Tian et al., J. Bacteriol. 187:3814–3824, 2005).

Polyhydroxybutyrates (PHBs) are biodegradable polymers with properties of thermoplastics synthesized by PHB synthases (PhaC) using (*R*)3-hydroxybutyryl coenzyme A as a substrate. In times of nutrient limitation, many bacteria generate these polymers when an appropriate carbon source is available (1). The soluble (*R*)3-hydroxybutyryl coenzyme A is transformed into insoluble polymers, called granules, in a nontemplate-dependent polymerization process (18). When the bacteria find themselves in a more hospitable environment, they degrade this polymer to generate building blocks and reducing equivalents for anabolism. However, bacteria in a nutrient-rich medium can also make and degrade PHB. The biology of PHB production and utilization under nutrient-rich conditions, however, remains to be elucidated.

The widespread detection of genes in many microorganisms that carry out PHB synthesis and degradation suggests that these pathways have evolved to be a general mechanism for bacterial cell survival in times of stress. The organism that we have chosen to study PHB homeostasis is *Wautersia eutropha* H16. This organism contains a class I synthase to generate PHB (15).

In this paper, we describe studies of PHB production and utilization by *W. eutropha* H16 in a nutrient-rich medium (dextrose-free tryptic soy broth [TSB]). Using antibodies (Abs) to most of the proteins identified as being involved in PHB homeostasis thus far, we carried out Western blotting as a function of growth time to measure the rates of appearance and disappearance of PhaC, PhaP (a phasin protein), and PhaR (a putative transcription factor), as well as PhaZ1$_a$, PhaZ1$_b$, PhaZ1$_c$, and PhaZ2 (formerly known as PhaZ1, PhaZ2, PhaZ3, and oligomer hydrolase, respectively); all of these proteins are thought to be involved in PHB degradation (10, 23). The average cell volume (20) and the average number of granules per cell at 4 and 24 h in TSB were determined by stereology analyses of transmission electron microscopy (TEM) images. These results and knowledge concerning the M_w of PHB allowed us to estimate the amount of each protein per cell, the percentage of the granule surface that is covered by PhaC and PhaP, and the number of PhaC molecules per PHB polymer. A comparison of these results with similar studies performed under nitrogen-limited growth conditions (unpublished data) provided insight into the requirements for granule formation and reutilization.

MATERIALS AND METHODS

Cultivation conditions. Wild-type *W. eutropha* and the Δ*phaR* deletion strain were cultivated in TSB using procedures described previously (23). Cells equivalent to an optical density at 600 nm (OD_{600}) of 5 were harvested at 0, 4, 8, 12,

* Corresponding author. Mailing address: Bldg. 18-598, Department of Chemistry, Massachusetts Institute of Technology, 77 Massachusetts Ave., Cambridge, MA 02139. Phone: (617) 253-1814. Fax: (617) 258-7247. E-mail: stubbe@mit.edu.

24, and 48 h. All cell samples collected were spun down, washed with a saline solution, and stored at −80°C for Western analysis.

Cell counting. Wild-type *W. eutropha* cells at zero time (containing ~15% PHB based on cell dry weight [CDW]) were counted three times (OD_{600}, 0.5) using a hemocytometer (Petroff-Hausser bacteria counter; Hausser Scientific, Horsham, PA), and the average cell number was used in the calculations. The cell pellet at zero time contained $\sim 7.1 \times 10^9$ cells. The volume of culture collected at each later time was adjusted to contain $\sim 7.1 \times 10^9$ cells based on the OD_{600}. The number of cells per ml of culture was assumed to be directly proportional to the OD_{600} of the culture. The variation in the PHB content in samples was assumed to have a minimal effect on the OD_{600} since the difference in the amount of PHB based on the CDW between zero time and other times sampled varied only from 0 to 15%.

Purification of Abs for Western analysis. Purification of $PhaZ1_a$, $PhaZ1_b$, and PhaR Abs will be described elsewhere (unpublished data). PhaC Ab was used as it was received from Covance Inc. (Princeton, NJ), and the PhaZ2 Ab was a kind gift from Terumi Saito (Kanagawa University, Japan).

Sample preparation for Western analysis. A cell pellet was thawed and resuspended in 500 μl of 50 mM Tris, 1 mM EDTA, 2% sodium dodecyl sulfate (SDS), pH 8. The cell suspension was sonicated using a microtip on an XL2020 sonicator (Misonix, Farmindale, NY) at power level 4 for 30 s (0.8 s on, 0.2 s off), and the sample was then heated at 95°C for 20 min before it was spun down at 13,000 rpm for 6 min. An appropriate amount of supernatant was chosen by trial and error for Western analysis to ensure that the signals observed were not saturated. Protein (600 to 1,200 ng) from crude lysate was loaded onto the gel. For detection of PhaC, PhaP, PhaR, $PhaZ1_a$, $PhaZ1_b$, and PhaZ2 in wild-type *W. eutropha*, amounts equivalent to 0.4, 0.4, 2, 0.4, 1, and 1 μl of the crude extract supernatant, respectively, were loaded. Recombinant PhaC, PhaP, PhaR, $PhaZ1_a$, and $PhaZ1_b$ overexpressed and purified from *Escherichia coli* were used to prepare standards; bovine serum albumin (0.1 mg/ml) and SDS (0.2%) were added to all standards. All Western analyses were carried out using standard procedures. Polyvinylidene difluoride membranes (Bio-Rad, Richmond, CA) were used for electroblotting. For PhaC, PhaR, and PhaZ2 Western analyses, 10%, 15%, and 10% Tris-Tricine gels (Bio-Rad), respectively, were used. The gels were blotted for 2.5 h at 50 V (PhaC and PhaR) or for 100 min at 80 V (PhaZ2) using a Criterion blotter (Bio-Rad). For PhaP, $PhaZ1_a$, and $PhaZ1_b$, 15%, 10%, and 10% self-made gels were used. These gels were blotted for 80 min at 100 V using a Mini Trans-Blot cell (Bio-Rad). The polyvinylidene difluoride membranes were then incubated with either anti-PhaC (dilution factor, 1/2,000), anti-PhaP (1/4,000), anti-PhaR (1/10,000), anti-$PhaZ1_a$ (1/10,000), anti-$PhaZ1_b$ (1/10,000), or anti-PhaZ2 (1/4,000) Ab for ~1 h. After appropriate washing procedures, the membranes were incubated with secondary Abs (goat anti-rabbit, conjugated with alkaline phosphatase) for ~45 min at appropriate dilutions. For PhaC and PhaR, signals were detected by using the Western-Light and Western-Star chemiluminescent detection systems (Applied Biosystems, Foster City, CA), respectively. For PhaP, $PhaZ1_a$, $PhaZ1_b$, and PhaZ2, signals were detected by using an Immuno-Star AP chemiluminescent kit (Bio-Rad). All Western images were recorded on a ChemiDoc XRS system and quantitated using Quantity One 1-D Analysis software (Bio-Rad).

Solubilization of proteins from PHB granules by SDS or using an extracellular PHB depolymerase. In order to determine whether 2% SDS can completely solubilize all proteins from the surface of PHB granules, two wild-type culture samples (1.7 ml) were collected at 4 h, when the maximum amount of PHB based on the CDW was produced. The cultures were spun down at 13,000 rpm for 3 min. After the supernatant was removed, the pellets were washed with 0.85% saline, followed by centrifugation. The pellets were stored at −80°C. To one pellet 0.5 ml of 2% SDS, 50 mM Tris, 1 mM EDTA, pH 8 (solubilizing buffer) was added to resuspend the cells. To the second pellet, 0.5 ml of the solubilizing buffer without SDS was added. Both cell suspensions were sonicated using conditions identical to those described above and then heated at 95°C for 20 min. The cell suspension from the first pellet was stored at 4°C until the next step. To the cell suspension from the second pellet, 20 μl (~0.1 U) of extracellular depolymerase isolated from *Pseudomonas lemoignei* (specific activity, 25 U/mg) in 50 mM Tris, 1 mM $CaCl_2$, 7.5% glycerol, pH 8, was added. An additional 5 μl of 100 mM $CaCl_2$ was also added so that the final $CaCl_2$ concentration was 1 mM. The reaction mixture was incubated at 37°C for ~12 h. The sample was then brought to 2% (final concentration) SDS and heated for 20 min at 95°C. The cell suspension from both pellets was spun down. Additional solubilizing buffer had to be added to the first pellet suspension so that its final volume was the same as that of the second pellet suspension. These supernatants were analyzed by Western blotting.

Extraction of PHB. At 4 h under the growth conditions described above, 10 ml of each culture was centrifuged (5,000 × *g*, 5 min) in a glass test tube, resuspended in 10 ml distilled water at 4°C, and centrifuged again (5,000 × *g*, 5 min), and the supernatant was decanted. The samples were lyophilized and extracted directly from the original test tubes by refluxing in 5 ml $CHCl_3$ for 48 h with stirring. Samples were then brought up to 5 ml in $CHCl_3$ and gravity filtered through Whatman no. 4 filter paper, and the tubes and filter were washed with 5 ml $CHCl_3$. The solvent (10 ml) was removed under N_2, and the samples were redissolved in 1 ml $CHCl_3$ (2 h, 25°C). The PHB was precipitated by addition of 3 ml methanol, and the precipitant was recovered by vacuum filtration using a Buchner funnel fitted with Whatman no. 474 filter paper. Filters were dried under reduced pressure (70×10^2 Pa) at 55°C for 24 h, at which time PHB was easily removed as a coherent film from each filter.

M_w determination. Each sample was dissolved in 2,2,2-trifluoroethanol (TFE) (Aldrich, St. Louis, MO) to obtain a final concentration of 1 mg PHB/ml. Dissolution took 24 h, after which an aliquot was removed and diluted to 0.25 mg PHB/ml in TFE and filtered through a 0.2-μm polytetrafluoroethylene (PTFE) filter (Pall, East Hill, NY). Coupled multiangle light scattering and gel permeation chromatography were used to determine the M_n and M_w of PHB. Light scattering was performed using a DAWN-EOS (λ, 690 nm) multiangle laser photometer (Wyatt Technology Corporation, Santa Barbara, CA). Gel permeation chromatography was carried out with a Knauer high-performance liquid chromatograph (Waters, Milford, MA) attached to a PLgel 10-μm Mixed-B column (Polymer Laboratories, Amherst, MA). A Wyatt Optilab DSP differential refractometer was used for quantitation of PHB, using a dn/dc value of 0.144. TFE was used as the mobile phase at a flow rate of 1.0 ml/min, and 100 μl of the sample was injected; 18.2-kDa narrow-molecular-mass poly(methyl-methacrylate) standards (catalog no. 602; dn/dc, 0.172; Scientific Polymer Products, Ontario, NY) were used to normalize the light scattering instrument, and other poly(methyl-methacrylate) standards (20 to 2,000 kDa) were used to confirm the calibration (catalog no. STD-4). Calculation of the molecular weight from light scattering was performed with the ASTRA software (Wyatt Technology) employing the Berry formalism.

Transmission electron microscopy. Five-milliliter portions of wild-type *W. eutropha* and the Δ*phaR W. eutropha* deletion strain were collected from the cultures described above at 4 h for TEM analysis. An additional wild-type cell sample was also collected at 24 h. The details of sample preparation for TEM analysis are described in the accompanying paper (20).

TEM data analysis. Since TEM images are essentially flat profiles of organelles obtained from random cuts through an embedded sample, the size of a profile is not representative of the size of the structures from which it arose. In order to be able to interpret the cell cross sections (cell profiles) in terms of three-dimensional structures, the TEM images of wild-type samples were analyzed using unbiased stereology (13). Point and intersection counting tests were designed to derive the average cell volume and average total surface area of granules per *W. eutropha* H16 cell. The detailed analysis is described in the accompanying paper (20).

Determination of the average number of granules per cell at 4 and 24 h in TSB using stereology. In order to determine the average number of granules per cell from two-dimensional TEM images by stereology, serial section images (~100 nm) from 4 and 24 h were generated and examined. The thickness of the sections for this analysis had to be less than the mean diameters of granules (20). We previously determined that these diameters were 0.36 μm and 0.24 μm at 4 and 24 h in TSB, respectively, assuming that all granules were a uniform size at each time. The methodology designed for estimation of the number of particles (e.g., number of granules) in a given tissue or specimen (e.g., cell) was developed by D. C. Sterio and is known as the Disector Principle (17). The first of a pair of disector probes (http://web.mit.edu/biochemistry/PHB_Supp_Z.pdf) is placed randomly over the first of two images of adjacent sections. The second probe is then placed on the corresponding area of the second image. The first probe serves as the reference section, while the second serves as the look-up section. Each granule present in the cell is counted only once by counting the granule profile at the initial intersection between the sectioning plane and the granule. In other words, granule profiles were counted only if they were present in the image of the reference section and not in the look-up section. In order to avoid overcounting, only granules present within the frame or on the inclusion lines were counted. This procedure was continued with images of other adjacent sections until the sampling error was less than 10% (here the number of samples was equal to the number of counting frames used). The total number of granules per unit volume of reference space (N_V) could be calculated using the following equation (17).

$$N_V = \Sigma Q^- / (\Sigma A \times h) \quad (1)$$

where ΣQ^- is the number of disappearing granules summed over all counting

frames, ΣA is the sum of the area of all counting frames, and h is the thickness of the section. Both ΣA and h had to be corrected by the magnification factor. This procedure was carried out for TSB samples collected at 4 and 24 h. This exercise provided the distribution of granules in the volumes defined by sets of serial sections.

However, the value determined in equation 1 gives the total number of granules in the reference space, which is not entirely filled with cells. Since we are interested in determining the number of granules per cell, we had to relate the volume occupied by cells in space to the reference volume, which is essentially volume of cells per reference space (V_V) (20). The average number of granules per cell (N_G) could be estimated using equation 2.

$$N_G = (N_V/V_V) \times V_C = (N_V/A_A) \times V_C \quad (2)$$

where V_V and A_A both refer to the cell and not to granule cross sections. The term N_V/V_V gives the average number of granules in the volume of cells in the same reference space. Therefore, if the average volume of one cell (V_C) is known, the average number of granules per cell can be obtained. The volume fraction is equal to the area fraction based on the Delesse principle, $V_V = A_A$. Determination of A_A and V_C is described in the accompanying paper (20).

In the accompanying paper (20), the methods used to determine the surface area of granules in reference space (S_V) and the surface area of all granules per cell (S_G) were described. Information concerning S_V and S_G allows N_G to be determined by an alternative method using equation 3.

$$N_G = S_G/(S_V/N_V) \quad (3)$$

where S_V/N_V gives the mean surface area of one granule. If S_G is known, the number of granules can be calculated.

RESULTS

Choice of TSB to study granule formation. As part of our effort to understand the mechanisms by which *W. eutropha* synthesizes and utilizes PHB, we studied the changes in protein levels involved in PHB homeostasis in different growth media as a function of time. The growth conditions in the present study included a nutrient-rich medium (TSB). Such conditions have received minimal attention as most efforts have been focused on maximizing PHB production, a process that requires growth under nutrient-limited conditions (12). In TSB, the levels of PHB increase from 15% to 23% of the CDW over the first 4 h of growth, and by 48 h, the PHB is completely degraded (23). The physiological reason for transient PHB production in TSB is presently not understood.

TSB was chosen to study transient PHB production and utilization based on our TEM observations shown in Fig. 1A and B. The images reveal that there were several small granules per cell, whose numbers could potentially be determined at 4 and 24 h. The granules at 24 h were also substantially smaller than those at 4 h (Fig. 1B), consistent with PHB degradation during this period. These images differ substantially from previous images of cells grown under nutrient-limited conditions, in which the concentration of granules was so large that the granules were the only visible structures within the cells (18). It is interesting that the cells grown in TSB did not make granules as large as those made by cells grown in nitrogen-limited conditions.

The 4-h TEM images were examined further by using serial sections, as shown in Fig. 2A through C. Examination of the features in the boxes in Fig. 2 and examination of the sections of hundreds of cells suggested that the granules within a cell are moderately uniform in size. The cells were dividing at this time (4 h), which provides an explanation for the heterogeneity in granule size occasionally observed among cells. At 24 h, most of the cells had entered the stationary phase, as indicated by the significantly reduced rate of increase in the $OD_{600\ nm}$ and the CDW with the weight of PHB subtracted (data not shown). At this time, the granules were very uniform.

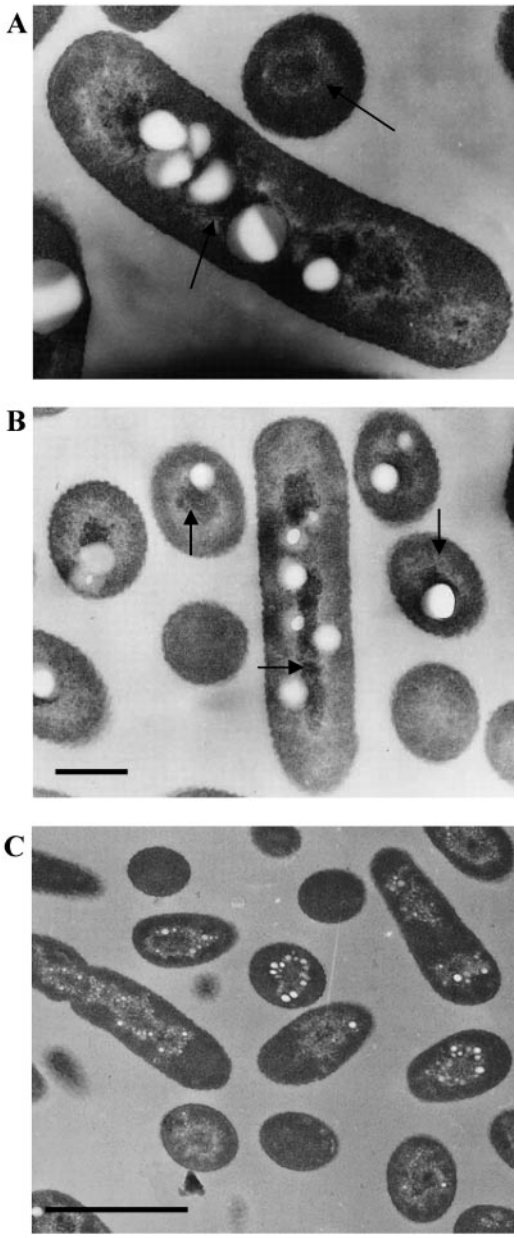

FIG. 1. (A and B) TEM images of wild-type *W. eutropha* H16 cells at 4 h (A) and 24 h (B), showing dark-stained structures (arrows). Bar, 500 nm for both panels A and B. (C) TEM image of Δ*phaR W. eutropha* H16 grown in TSB for 4 h, showing localization of small granules. Bar, 1.9 μm.

Determination of the average number of granules per cell at 4 and 24 h in TSB. To determine the number of granules within a cell, one needs to know either the average cell volume or the average total surface area of granules per cell. Unbiased stereology has recently been used to estimate each of these values for *W. eutropha* H16 grown in TSB at 4 and 24 h (20). At 4 h, ranges of V_C and S_G values were determined based on the observation that the cells were dividing during this time. The

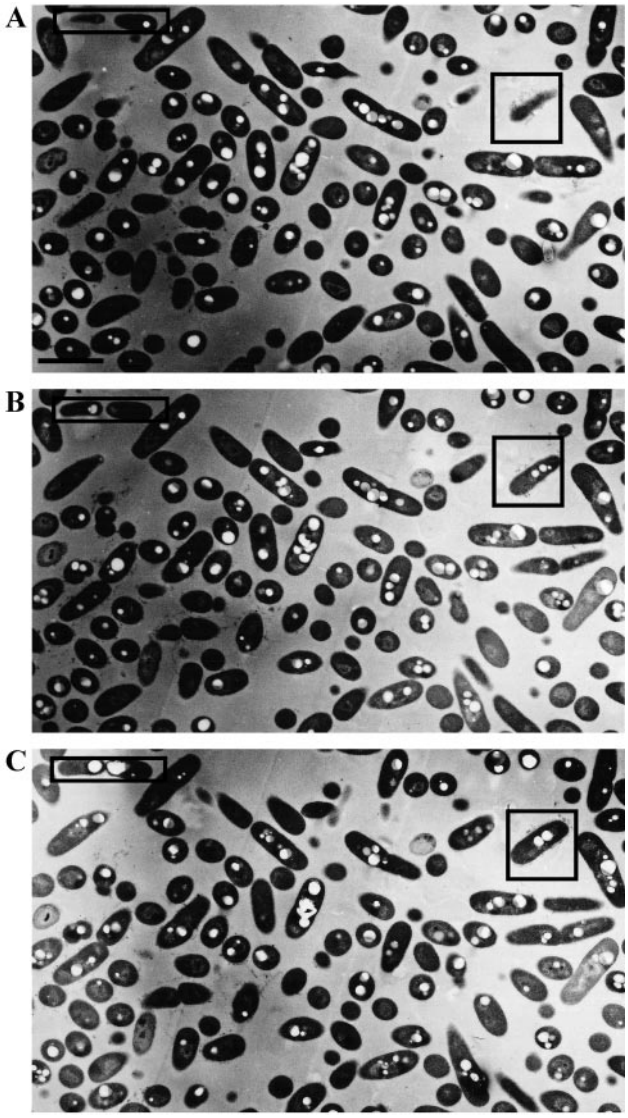

FIG. 2. TEM images of consecutive serial sections of wild-type strain *W. eutropha* H16 grown in TSB for 4 h. Bar, 2 μm.

range for cell volumes was from 0.9 μm^3 to 1.8 μm^3; the former value was associated with cells that had newly undergone cell division, and the latter value was associated with cells immediately before cell division. Thus, 0.9 μm^3 and 1.8 μm^3 were the minimum and maximum cell volumes at this time, and the average cell volume of the entire population of cells was within this range. For similar reasons, an S_G range (1.3 to 2.5 μm^2) was also determined. The V_C and S_G at 24 h obtained from stereological analysis provided close estimates of the cell volume and granule surface area of the actual population of cells as the cells were close to stationary phase.

With this information, the average number of granules per cell could be extracted from the images of serial sections (Fig. 2) using the dissector probe based on the Disector Principle (17). By counting the total number of disappearing granule profiles from the reference section to the look-up section in a known reference volume, the average number of granules per cell could be calculated by two methods (see equation 2 and equation 3 in Materials and Methods). The first method related the number of granules per reference space (N_V) to the volume of cells per reference space (V_V) and used the information concerning the average cell volume (V_C) to obtain the average number of granules per cell (N_G). The second method used the average surface area of one granule (S_V/N_V) and S_G to obtain N_G. The results of the two methods agree. There were approximately five granules per *W. eutropha* H16 cell at 24 h in TSB. At 4 h, there were two or three granules per cell if the average volume of the freshly divided cells was used and ~five granules per cell if the average volume of the elongated cells before cell division was used. The number of granules was substantially reduced from the number reported for cells grown in nutrient-limited media (1, 20).

Quantitative Western analysis. As a first step in our Western analysis to determine the concentrations of various proteins and changes in these concentrations during transient PHB production, we used Abs to PhaC, PhaR, PhaP, $PhaZ1_a$, $PhaZ1_b$, $PhaZ1_c$, and PhaZ2. In the case of PhaR, PhaP, $PhaZ1_a$, $PhaZ1_b$, and $PhaZ1_c$, the Abs were generated from purified proteins and further purified using the corresponding deletion strains. PhaC Abs required no additional purification, and Abs to PhaZ2 were used without further purification (10). Many of these proteins at some point are attached to the PHB granules (6, 10, 21), and we worried about our ability to remove these proteins quantitatively. Thus, a set of controls in which extracellular depolymerase was used to remove PHB (see Materials and Methods) demonstrated that boiling the crude cell extracts in 2% SDS for 20 min at 95°C was sufficient to recover all of the protein in the cell regardless of its location (data not shown).

Analysis of proteins in wild-type *W. eutropha H16*. The changes in protein amounts as a function of growth conditions were examined by quantitative Western blotting methods. The results of a typical set of experiments are shown in Fig. 3. In addition, we chose to express the amount of each protein in fmol/μl of cell extract. During the sample collection process designed to compensate for increased cell number, a smaller volume of culture was used for cell isolation by centrifugation (see Materials and Methods). The decision to do this was based on the assumption that the number of cells per ml of culture was directly proportional to the OD_{600} in TSB. Each pellet should therefore have contained the same number of cells. This method assumed that the change in optical density was a good reflection of the change in cell number. We believe that this is a good assumption as the cells did not make a large amount of PHB under these growth conditions. The error associated with the volume used to collect cells based on the optical density was <10%, which is less than the error associated with cell counting (20 to 30%). By resuspending each cell pellet with the same volume of buffer, the amount of each protein at a given time could be compared in terms of fmol/μl of cell extract. Figure 3B shows the relative amount of each protein as a function of time in the wild-type strain.

Relationship between PhaP and PHB. Previous studies have demonstrated that increasing amounts of PhaP occur with increased PHB production (22). Figures 3A and B show the first kinetic correlation between these two species. The rate at which PHB was produced and utilized correlated with the rate at which PhaP was produced and degraded.

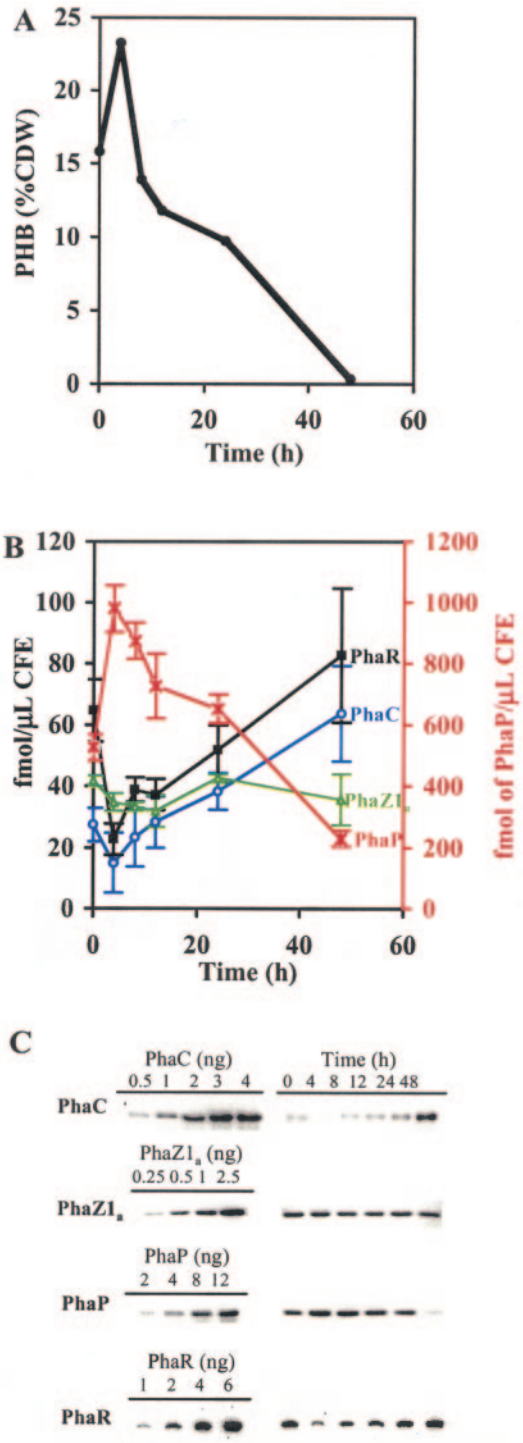

FIG. 3. (A) Profile of PHB accumulation by wild-type strain *W. eutropha* H16 in TSB. (B) Expression of PhaC, PhaP, PhaR, and PhaZ1$_a$ in wild-type *W. eutropha* from 0 to 48 h in TSB. Note that the scale for PhaP on the right is different from the scale for the other proteins on the left. (C) Western blots of PhaC, PhaP, PhaR, and PhaZ1$_a$ from crude extracts of wild-type *W. eutropha*. Western blots compared to standards were used to generate the data in panel B.

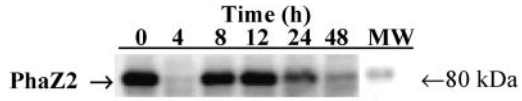

FIG. 4. Western blot of oligomer hydrolase for the wild-type *W. eutropha* H16 strain. MW, molecular weight.

Time course for PhaC, PhaR, and PhaZ1$_a$. The amounts of PhaC, PhaR, and PhaZ1$_a$ did not appear to change appreciably between 0 and 12 h (Fig. 3), and these proteins were constitutively expressed. The slight downward trend in the amounts of PhaC and PhaZ1$_a$ from 0 to 4 h may reflect the error associated with the assumption that OD_{600} is proportional to cell number. The amount of PHB/ml of cell culture increased from 0.03 mg to 0.14 mg between 0 to 4 h, and the additional amount of PHB increased the OD_{600} by ~0.2. The downward trend in the amount of PhaR from 0 to 4 h is much more significant than the trend for PhaC and PhaZ1$_a$. Between 12 and 48 h, the amounts of PhaC and PhaR increased. From 4 to 48 h, all of the PHB was degraded, indicating that the amount of carbon in the medium was small. Other metabolites could also have been limiting such that cells were stressed and consequently were preparing themselves to produce more PHB. As a result, PhaC and PhaR expression could have been upregulated, and the cells could have been ready to make PHB when the appropriate nutrient conditions were encountered.

Are the synthase and depolymerases present simultaneously? Current genetic evidence supports the involvement of at least three proteins (PhaZ1$_a$, PhaZ1$_b$, and PhaZ2) in the depolymerization process (10, 23). Western analyses were carried out using PhaZ1$_a$, PhaZ1$_b$, PhaZ1$_c$, and PhaZ2 Abs for each sample (Fig. 3B and C and 4) to determine if the proteins were present and how the concentrations changed during the analysis period. PhaZ1$_a$ was present in the presence and absence of PHB. Neither PhaZ1$_b$, nor PhaZ1$_c$ was detected at the times sampled (data not shown), suggesting that they are not involved in PHB production and degradation under these growth conditions. The absence of PhaZ1$_b$ contrasts with the results of similar experiments carried out under nitrogen-limited growth conditions (unpublished data).

PhaZ2, the hydroxybutyrate oligomer hydrolase and a putative PHB intracellular depolymerase, was recently discovered by Kobayashi and coworkers (10). Our Western analysis revealed that the expression pattern of PhaZ2 (Fig. 4) was different from that of PhaZ1$_a$ (Fig. 3C). At present, we have not yet purified this protein, and consequently a standard curve is not available to determine the amount of PhaZ2; only changes in its levels with time can be monitored. The PhaZ2 levels increased from 4 to 12 h and decreased substantially with the disappearance of PHB. In contrast, the PhaZ1$_a$ concentrations were relatively constant over the entire time. Kobayashi et al. proposed that the synthesis of PhaZ1$_a$ and PhaZ2 are stringently correlated with PHB production under similar nutrient-rich conditions (10). Our data (Fig. 3 and 4) show that this is not the case in TSB.

In vivo concentrations and number of molecules per cell for PhaC, PhaP, PhaR, and PhaZ1$_a$ at 4 and 24 h in TSB. Quantitative Western analysis provided information about the amount of each protein in the cells. In the accompanying

TABLE 1. In vivo concentrations and numbers of molecules of PhaC, PhaP, PhaR, and $PhaZ1_a$ in wild-type *W. eutropha* strain H16 at 4 and 24 h in TSB, assuming that all proteins were soluble

Protein	4 h in TSB		24 h in TSB	
	Concn (μM)	No. of molecules per cell	Concn (μM)	No. of molecules per cell
PhaC	0.3–0.6	3.3×10^2	2.6	1.4×10^3
PhaP	36–72	3.9×10^4	48	2.6×10^4
PhaR	1–2	1.1×10^3	4.5	2.4×10^3
$PhaZ1_a$	1.4–3	1.5×10^3	3.2	1.8×10^3

paper, the average cell volumes of a *W. eutropha* H16 cell at 4 and 24 h in TSB are reported to be 0.9 to 1.8 μm^3 and 0.9 μm^3, respectively (20). Knowing the number of cells and the amount of each protein that the cells contain allowed calculation of the concentration of each protein and the number of molecules of each protein per cell. The results are summarized in Table 1. The choice to report the concentrations (μM) of each protein assumed that the proteins are soluble and are not localized to granules or membranes. Since different populations of cells were present at 4 h in TSB, ranges for the protein concentrations or the number of protein molecules per cell are reported for this time. The ratio of $PhaZ1_a$ to PhaC was approximately 5:1 at 4 h and 1:1 at 24 h. Also of interest is the ratio of PhaR to PhaC (2:1). The concentration of PhaR is particularly striking as PhaR is a regulatory protein. The levels of PhaR and the close stoichiometry relative to PhaC suggest that it plays a role other than the role of a transcription factor. Finally, PhaP was present at a much higher concentration (~40 μM) than the rest of the proteins studied, consistent with reports of other workers (21).

Protein coverage of the granule surface area of each cell at 4 and 24 h in TSB. Previous immunogold labeling experiments have shown that PhaC and PhaP are located on the granule surface under nitrogen-limited conditions (6, 14). The amount of PhaP produced under these conditions has been estimated to be 3 to 5% of the total amount of protein present (21). Results from the present studies indicate that PhaP accounted for ~9% of the total amount of protein present at 4 h in TSB. At present, no information is available on the location of PhaC and PhaP under nutrient-rich conditions. For calculation purposes, we assumed that both proteins are granule bound. Using this assumption, the extent of granule surface coverage by PhaC and PhaP could be calculated. The calculation required knowledge that the average total surface areas of granules per cell (S_G) determined by stereology at 4 and 24 h in TSB were 1.3 to 2.5 μm^2 and 1.3 μm^2, respectively (20). Assuming that PhaP (20 kDa) and PhaC (64 kDa) are both globular, the Stokes radii (R) of the two proteins could be estimated to be 2.1 nm and 3.5 nm, respectively, using chymotrypsinogen A (25 kDa) and bovine serum albumin (66 kDa), which are globular proteins of comparable sizes, as models. From the size, one can estimate the theoretical number of each of these proteins required to cover the entire surface of granules per cell. In this calculation, we assumed that the area of the protein that is in contact with the granule is equivalent to the area of a square with the length of each side equal to the diameter of the globular protein (area = $[2 \times R]^2$). Dividing the total surface area of granules in a cell by this contact area gave the approximate maximum number of each protein molecule that could occupy the surface of the granules (Table 2). Since we know the amount of protein extracted from a known number of cells, the actual number of PhaC molecules and PhaP molecules per cell could be obtained (Table 1). A comparison of the experimentally determined number and the estimated maximum gave ranges of protein coverage at 4 h due to the complications associated with cell division. At 4 h, there were approximately 330 molecules of PhaC and 39,000 molecules of PhaP per cell. The total surface area of granules per cell was 1.3 μm^2 to 2.5 μm^2, and the levels of coverage by PhaC and PhaP were 1.6% to 0.8% and 54% to 27%, respectively (Table 2). Similar values for PhaP surface coverage (35%) were obtained for cells at 24 h. However, the PhaC coverage increased significantly between 4 and 24 h from 0.8 to 1.6% to 5.5% due to the increasing amount of PhaC and the decrease in the total granule surface area per cell. The low surface coverage for PhaP suggests that the granules formed under TSB conditions are likely covered by lipid or other unknown components.

M_w of PHB at 4 h in TSB allows determination of the PhaC/PHB and PhaP/PHB ratios: evidence for reinitiation of PHB biosynthesis. The molecular mass of PHB was determined by dynamic light scattering to be 1.05 MDa (polydispersity, 1.2). This number, the amount of PHB in a given volume of cell culture (8), and the amount of PhaC (as determined by Western analysis) allowed calculation of the ratio of the number of molecules of PHB to the number of molecules of PhaC, which was ~60. This result required that PhaC can reinitiate polymer formation. The low polydispersity of the PHB molecular weight suggests that this process is exquisitely controlled by either PhaC itself or by PhaC in conjunction with other factors, such as PhaP or perhaps PhaR. The ratio of PhaP to PHB was similarly calculated to be 1 to 2. This number has important implications in establishing a function for PhaP in granule biogenesis.

TABLE 2. Protein coverage of the granule surface at 4 h

Time (h)	No. of PhaC molecules			No. of PhaP molecules		
	Theoretical[a]	Expt 1[b]	%[c]	Theoretical[a]	Expt 1[b]	%[c]
4	2.5×10^4–5.1×10^4	3.3×10^2	0.8–1.6	0.7×10^5–1.4×10^5	3.9×10^4	27–54
24	2.7×10^4	1.4×10^3	5.5	7.4×10^4	2.6×10^4	35

[a] Theoretical number of protein molecules covering the total surface area of granules per cell. Note that for 4 h, a range is given due to the complications associated with cell diviosn; the total surface area of granules in a freshly divided cell is one-half that in an elongated cell before cell division.
[b] Experimental number of protein molecules covering the total surface area of granules per cell.
[c] Experimental/theoretical × 100.

Localization of granules observed in the Δ*phaR W. eutropha* strain. Our recent kinetic studies of wild-type *W. eutropha* grown in nitrogen-limited medium using TEM revealed nascent granules localized on dark-stained mediation elements near the center of the cell in the early stages of granule biosynthesis (20). Similar structures were apparent at 4 and 24 h in TSB (Fig. 1A and 1B) analyzed by a similar procedure. TEM studies of a Δ*phaR* strain grown in TSB (4 h) also revealed small granules localizing near the center of the cell (Fig. 1C). The increased number of small granules is similar to the phenotype of the same strain grown under nutrient-limited conditions (14).

DISCUSSION

Studies of PHB production and utilization under TSB conditions have provided new insight into granule formation and PHB degradation. First, the kinetics of PhaP formation and disappearance are closely coupled to PHB levels, and there are one or two PhaP molecules/PHB polymer at 4 h. While previous studies have demonstrated unequivocally the importance of PhaP in PHB formation, a kinetic correlation and the relative amounts of PhaP and PHB have not been established previously.

Second, both PhaC and $PhaZ1_a$ are detected throughout TSB cultivation. Both of these proteins are constitutively expressed, and they are present in similar amounts. Comparison of our results with those recently reported by the Saito group revealed some discrepancies which may be associated with differences in sampling times and analysis methods. While Kobayashi et al. detected the presence of $PhaZ1_a$ in nitrogen-starved, carbon-rich medium (10, 16), they failed to detect the presence of $PhaZ1_a$ in nutrient-rich medium similar to TSB. They also claimed that under nutrient-limited conditions, the ratio of $PhaZ1_a$ to PhaC was 1:500 (10). The amount of $PhaZ1_a$ in their experiments was determined by Western analysis. The amount of PhaC (18,000 molecules per cell) was obtained from previous work (9). Quantitative Western analysis in our studies revealed that the ratios of $PhaZ1_a$ to PhaC are close to 5:1 at 4 h and 1:1 at 24 h in TSB. Similar ratios have also been found in cells grown in nitrogen-limiting conditions (unpublished data).

Third, it is also clear from our studies that PhaC and $PhaZ1_a$ are present during the entire growth period in TSB. It is not possible to tell, however, if the synthase and the depolymerase are active at the same time. Previous studies of Doi et al. (4, 9) and more recent studies of Saito et al. (10, 16) have been interpreted to support the simultaneous presence of an active synthase and a depolymerase(s). The results of Doi et al. are compelling, but these workers examined cells in the stationary phase, in contrast to TSB conditions (4). Studies of Kobayashi et al. on a Δ*phaZ1*$_a$*phaZ2* double deletion strain of *W. eutropha* H16 showed that more PHB was accumulated by this strain at the log phase under nutrient-rich conditions than by the wild-type strain under the same conditions. Thus, three independent lines of evidence support the simultaneous presence of a synthase and a depolymerase(s). However, the regulation of these activities remains an unresolved issue.

Fourth, our preliminary studies with PhaZ2 showed that its kinetics of appearance and disappearance differ from those of $PhaZ1_a$ and suggest that the two proteins have different functions. $PhaZ1_a$ is present during PHB production and hence might be involved in remodeling the granule, while PhaZ2 is most prevalent during degradation. Interestingly, neither $PhaZ1_b$ nor $PhaZ1_c$ has been detected under TSB growth conditions, nor have their biochemical functions been accessible in vitro.

Granule characterization in TSB. We also determined the average number of granules per cell at 4 and 24 h in TSB. A change in cell size due to cell division complicates the analysis at 4 h. The fate of the granules during cell division (that is, whether they are equally distributed between daughter cells) is not known. Given this problem and consequently assuming a range of cell volumes and total granule surface per cell, using unbiased stereology we calculated that there are two to five granules per cell. At 24 h when the cells are more uniform and not dividing, there are five granules per cell. The average size of the granule (Fig. 1A and B) also decreases, and the degradation of the granules appears to be uniform.

TEM studies of the *W. eutropha* wild-type strain and the Δ*phaR* deletion strain grown in TSB conditions provided additional support for a new model for granule formation that we propose in the accompanying paper (20). These studies revealed that the granules were localized on dark-stained mediation elements near the center of the cells and suggested that biology plays a much more important role in nucleation of granule formation than previously anticipated.

The mediation elements and granule localization were again observed in 4- and 24-h TEM samples (Fig. 1A and B), although they were less readily apparent at 4 h. The localization of granules in these images and in the TEM image of the Δ*phaR* strain grown in TSB (Fig. 1C) is apparent, although in the latter image, the presence of mediation elements is not apparent. The TEM results for TSB are at odds with the micelle model and membrane budding model of granule formation (5, 18).

Granule formation was further elucidated by our determination that 27 to 54% of the granule surface is covered with PhaP. Previous electron microscope studies of PHB granules from *Bacillus cereus*, *Bacillus megaterium* (11), *Rhodospirillum rubrum* (2), and *Chlorogloea fristschii* (7) all agree on the presence of a layer surrounding the surface of granules. The size of the layer (3 to 20 nm), however, appears to be species dependent. These studies, along with biochemical analysis of changes in the amounts of lipid during PHB production (19), suggest that a monolayer of lipid might be involved in surface coverage of granules. Recent atomic force microscopy analyses suggested that there is a structure on the granule surface that is 350 Å in diameter and has a 150-Å pore-like structure in the center (3). Clearly, more careful analysis using multiple techniques is required to understand the biology of granule formation.

Finally, the mechanism of PHB chain termination is of great interest for development of new material. We have calculated that at the maximum percentage of PHB based on the CDW (4 h), there are approximately 60 PHB chains per PhaC molecule, and our measurements have shown that the PHB is amazingly monodisperse. Given that the polymerization process involves covalent catalysis, the polymer must be hydrolyzed or undergo transesterification prior to reinitiation. Understanding the role

of PhaC, the role of one or two PhaP molecules per PHB chain, and the role of PhaR that is present in amounts similar to the amounts of PhaC in this reinitiation process is a major focus of our efforts.

ACKNOWLEDGMENTS

This work was supported by NIH grant GM49171 to JoAnne Stubbe and Anthony J. Sinskey and by NIH training grant 5T32GM08334 to Jiamin Tian.

We thank Peter Mouton (Stereology Resource Center, Inc., and Stereology Laboratory at the Laboratory of Neurosciences Gerontology Research Center, NIA/NIH, Baltimore, Md.) for providing the disector probe and for helpful discussions concerning stereological analysis.

REFERENCES

1. **Anderson, A. J., and E. A. Dawes.** 1990. Occurrence, metabolism, metabolic role, and industrial uses of bacterial polyhydroxyalkanoates. Microbiol. Rev. **54:**450–472.
2. **Boatman, E. S.** 1964. Observations on the fine structure of spheroplasts of *Rhodospirillum rubrum*. J. Cell Biol. **20:**297–311.
3. **Dennis, D., C. Liebig, T. Holley, K. S. Thomas, A. Khosla, D. Wilson, and B. Augustine.** 2003. Preliminary analysis of polyhydroxyalkanoate inclusions using atomic force microscopy. FEMS Microbiol. Lett. **226:**113–119.
4. **Doi, Y., A. Segawa, Y. Kawaguchi, and M. Kunioka.** 1990. Cyclic nature of poly(3-hydroxyalkanoate) metabolism in *Alcaligenes eutrophus*. FEMS Microbiol Lett. **55:**165–169.
5. **Ellar, D., D. G. Lundgren, K. Okamura, and R. H. Marchessault.** 1968. Morphology of poly-beta-hydroxybutyrate granules. J. Mol. Biol. **35:**489–502.
6. **Gerngross, T. U., P. Reilly, J. Stubbe, A. J. Sinskey, and O. P. Peoples.** 1993. Immunocytochemical analysis of poly-β-hydroxybutyrate (PHB) synthase in *Alcaligenes eutrophus* H16: localization of the synthase enzyme at the surface of PHB granules. J. Bacteriol. **175:**5289–5293.
7. **Jensen, T. E., and L. M. Sicko.** 1971. Fine structure of poly-beta-hydroxybutyric acid granules in a blue-green alga, *Chlorogloea fritschii*. J. Bacteriol. **106:**683–686.
8. **Karr, D. B., J. K. Waters, and D. W. Emerich.** 1983. Analysis of poly-beta-hydroxybutyrate in *Rhizobium japonicum* bacteroids by ion-exclusion high-pressure liquid-chromatography UV detection. Appl. Environ. Microbiol. **46:**1339–1344.
9. **Kawaguchi, Y., and Y. Doi.** 1992. Kinetics and mechanism of synthesis and degradation of poly(3-hydroxybutyrate) in *Alcaligenes eutrophus*. Macromolecules **25:**2324–2329.
10. **Kobayashi, T., M. Shiraki, T. Abe, A. Sugiyama, and T. Saito.** 2003. Purification and properties of an intracellular 3-hydroxybutyrate-oligomer hydrolase (PhaZ2) in *Ralstonia eutropha* H16 and its identification as a novel intracellular poly(3-hydroxybutyrate) depolymerase. J. Bacteriol. **185:**3485–3490.
11. **Lundgren, D. G., R. M. Pfister, and J. M. Merrick.** 1964. Structure of poly-beta-hydroxybutyric acid granules. J. Gen Microbiol. **34:**441–446.
12. **Madison, L. L., and G. W. Huisman.** 1999. Metabolic engineering of poly(3-hydroxyalkanoates): from DNA to plastic. Microbiol. Mol. Biol. Rev. **63:**21–53.
13. **Mouton, P. R.** 2002. Principles and practices of unbiased stereology: an introduction for bioscientists. The Johns Hopkins University Press, Baltimore, Md.
14. **Potter, M., M. H. Madkour, F. Mayer, and A. Steinbuchel.** 2002. Regulation of phasin expression and polyhydroxyalkanoate (PHA) granule formation in *Ralstonia eutropha* H16. Microbiology **148:**2413–2426.
15. **Rehm, B. H., and A. Steinbüchel.** 1999. Biochemical and genetic analysis of PHA synthases and other proteins required for PHA synthesis. Int. J. Biol. Macromol. **25:**3–19.
16. **Saegusa, H., M. Shiraki, C. Kanai, and T. Saito.** 2001. Cloning of an intracellular poly[D(−)-3-hydroxybutyrate] depolymerase gene from *Ralstonia eutropha* H16 and characterization of the gene product. J. Bacteriol. **183:**94–100.
17. **Sterio, D. C.** 1984. The unbiased estimation of number and sizes of arbitrary particles using the disector. J. Microsc. **134:**127–136.
18. **Stubbe, J., and J. Tian.** 2003. Polyhydroxyalkanoate (PHA) homeostasis: the role of PHA synthase. Nat. Prod. Rep. **20:**445–457.
19. **Thiele, O. W., J. Dreysel, and D. Hermann.** 1972. The "free" lipids of two different strains of hydrogen-oxidizing bacteria in relation to their growth phases. Eur. J. Biochem. **29:**224–236.
20. **Tian, J., A. J. Sinskey, and J. Stubbe.** 2004. Kinetic studies of polyhydroxybutyrate granule formation in *Wautersia eutropha* H16 by transmission electron microscopy. J. Bacteriol. **187:**3814–3824.
21. **Wieczorek, R., A. Pries, A. Steinbüchel, and F. Mayer.** 1995. Analysis of a 24-kilodalton protein associated with the polyhydroxyalkanoic acid granules in *Alcaligenes eutrophus*. J. Bacteriol. **177:**2425–2435.
22. **York, G. M., B. H. Junker, J. A. Stubbe, and A. J. Sinskey.** 2001. Accumulation of the PhaP phasin of *Ralstonia eutropha* is dependent on production of polyhydroxybutyrate in cells. J. Bacteriol. **183:**4217–4226.
23. **York, G. M., J. Lupberger, J. Tian, A. G. Lawrence, J. Stubbe, and A. J. Sinskey.** 2003. *Ralstonia eutropha* H16 encodes two and possibly three intracellular poly[D-(−)-3-hydroxybutyrate] depolymerase genes. J. Bacteriol. **185:**3788–3794.